Sound & Vibration 2025, 59(1), 2073.
https://doi.org/10.59400/sv2073

Article

Sound insulation prediction and optimization of wooden support structure for high-speed train floor based on machine learning

Haiyang Ding[1], Ruiqian Wang[1,2,*], Xuefei Zhang[1], Ziyan Xu[1], Ancong Zhang[1], Lei Xu[3]

[1] School of Mechanical Engineering and Rail Transit, Changzhou University, Changzhou 213164, China
[2] Southwest Jiaotong University Changzhou Institute of Railtransport, Changzhou 213164, China
[3] CRRC Qishuyan Institute Co., Ltd., Changzhou 213000, China
*** Corresponding author:** Ruiqian Wang, ruiquanwang@163.com

CITATION

Ding H, Wang R, Zhang X, et al. Sound insulation prediction and optimization of wooden support structure for high-speed train floor based on machine learning. Sound & Vibration. 2025; 59(1): 2073. https://doi.org/10.59400/sv2073

ARTICLE INFO

Received: 23 July 2024
Accepted: 13 November 2024
Available online: 19 December 2024

Abstract: In order to improve the sound insulation performance of high-speed train floors, this study first obtained the necessary data for model training based on the reverberation test method, and then conducted data sorting and feature selection. Next, the maximum mutual information minimum redundancy (mRMR) feature selection algorithm was used to calculate the selected features and screen out a subset of significant features. Subsequently, the decision tree, BP neural network, and support vector machine regression (SVR) methods were applied in sequence, and the standardized feature data were used for the high-speed train floor under the same evaluation criteria of the mean square error (*MSE*) and coefficient of determination (R^2). We conducted training and validation of the sound insulation prediction models for timber-framed support structures. The prediction accuracy of the trained model was compared and evaluated with the finite element statistical energy analysis (FE-SEA) prediction model. Finally, the SVR model was used to optimize the design under constraint conditions. The research results show that based on the research object, sample library, and model training in this article, compared with the FE-SEA model, the prediction error of the SVR model is only 0.3 dB, showing better performance. In engineering practice, the SVR model can effectively optimize the wooden support structure in the floor under certain constraints, and it predicts that the weighted sound insulation of the entire floor is 50.45 dB, which has important engineering application value.

Keywords: high-speed train; floor wooden support structure for floor; sound insulation prediction; machine learning; optimized design

1. Introduction

As the running speed of high-speed trains continues to increase, the noise inside and outside the train increases sharply, and a large amount of noise enters the train through the train body, especially the frequency band of 100 Hz-2000 Hz, seriously affecting the ride comfort of drivers and passengers [1–7]. In this context, a high-speed train's floor structure, which is adjacent to the under-vehicle wheel rail area, is the most important way for noise to propagate from the outside to the inside in the airborne sound transmission path, so improving the sound insulation characteristics of this structure to reduce the impact of the under-vehicle noise on the interior of the vehicle is a direct and effective way to improve the acoustic environment inside the vehicle [8–11].

The floor structure is different from the side wall structure, front structure, end wall structure, etc. The wooden support structure is an indispensable part of the floor structure and accounts for a large proportion of the entire floor structure, as shown in

Figure 1. Among them, the interlayer material layer is the main area used to lay sound insulation, sound absorption and damping materials. By trying to add and replace materials, a structure with better sound insulation can be obtained. At present, the use of wooden support structures in high-speed train floors has not been fully investigated, especially in terms of sound insulation performance.

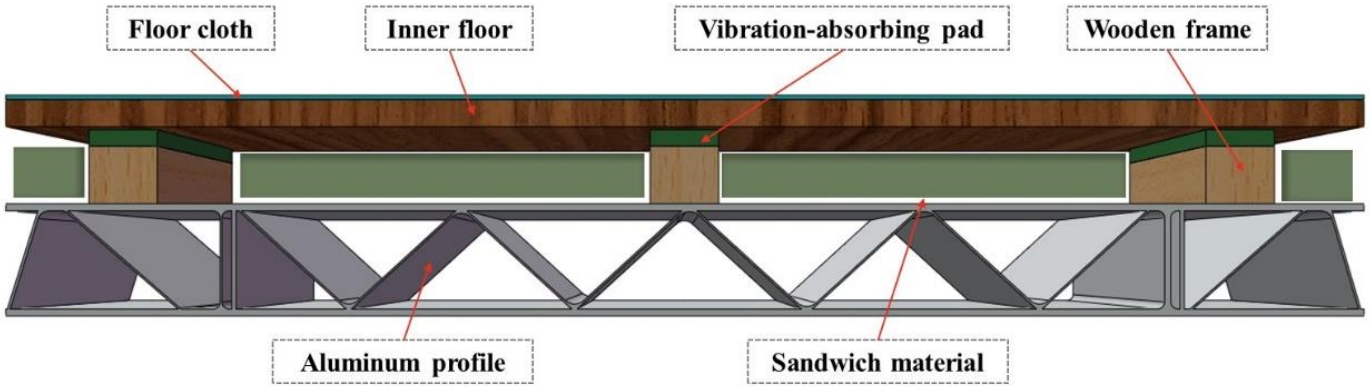

Figure 1. Diagram of common floor structures in high-speed trains.

Traditional floor structure sound insulation prediction and optimization are usually carried out through two methods: testing and simulation [12]. The former is mostly based on multiple on-site assembly tests and comparisons to obtain test data. This places high demands on laboratories and various materials, and the test costs are relatively high. Han measured the mechanical properties of different composite multi-layer floorings and calculated the mechanical property parameters of multi-layer floor materials based on the measurement results [13]. Kim studied aluminum extrusion panels for 400 km/h trains and proposed a practical method to improve the sound insulation performance by modifying the core structure to increase the local resonance frequency area and placing polyurethane foam in the core. Experiments verified the impact on the sound insulation effect [14]. Wang investigated the impact of altering the sequence of materials and structures, confirming through sound insulation tests that concentrating sound-absorbing materials in the middle, with sound-insulating materials on either side, improves the mid-frequency sound insulation performance. This approach was subsequently applied to optimize the sound insulation of high-speed train car bodies [15]. Zhang utilized two methods—on-site measurement and simulation analysis—to verify the vibroacoustic model of composite flooring and assess the contribution of its constituent materials. The results indicate that effective noise and vibration control of composite flooring should prioritize the design of the wooden keels, including aspects such as their quantity, arrangement, and material [16]. Yao selected water-based vibration-damping coating as a good noise reduction and vibration reduction material, and proposed a modal adaptive damping treatment optimization design for floor structures, which is widely used in railway floor structures and greatly reduces the overall radiated sound power of the floor [17].

The latter are mostly based on modeling and calculations based on the finite element [18] or statistical energy method [19] or algorithms [20] (genetic algorithm [21,22], particle swarm algorithm [23,24]), which have higher

requirements for model accuracy and material parameter investigation. Zhang carried out a comprehensive statistical energy analysis (SEA) and contribution analysis of the internal noise in high-speed trains. The study identified that, for the passenger car examined, the primary contributors to internal noise were side wall vibrations, noise from the bogie area, and floor noise transmission loss [25]. Xie established a simulation model of the acoustic properties of aluminum profiles based on statistical energy analysis (SEA). The research results show that under force load excitation, the prediction results of the SEA model are relatively close to the test results [26]. Cotoni established a hybrid FE-SEA model for high-speed train floors with corrugated aluminum profiles and verified the model through numerical methods [27]. Kim predicted the sound insulation characteristics of aluminum profile structures based on the finite element method, verified the simulation prediction model based on test results, and investigated the effects of boundary conditions and damping loss factors on the sound insulation amount [28]. Yu established a noise prediction model at the end of the cabin structure based on the FE-SEA hybrid method to predict the noise level in the cabin and analyze the sound energy contribution of key components in the cabin [29]. Yan used genetic algorithms to optimize phononic crystal plates to achieve a lightweight and ultra-wide bandgap [30].

However, with the rapid advancement of artificial intelligence, machine learning, as its core technology, has progressively permeated various fields [31–34]. Wang developed a machine learning model using the random forest method to predict the sound insulation performance of composite floors and identified the key factors influencing this performance. The results indicate that, considering all material properties, the sound insulation of aluminum profiles, the surface density, and the sound insulation of interior wall panels are the three most significant factors affecting the sound insulation of composite flooring [35]. Sahib employed the Non-dominated Sorting Genetic Algorithm (NCGA) to explore the design space of fiber metal laminates (FMLs) and utilized the finite element method (FEM) to develop the optimal design for train carriage floors. The results showed that the manufactured panels can significantly reduce the weight of the floor [36].

Section 2 mainly outlines the research process and methods. Section 3 focuses on the source of samples and how to select sample features. Section 4 explains the preparations that need to be carried out before model training, especially the use of the mRMR feature selection algorithm for feature screening. Section 5 uses the decision tree, BP neural network, and support vector machine regression methods to train and verify the prediction model for the sound insulation performance of high-speed train floor structures using standardized feature data. The trained model is analyzed and compared with the FE-SEA simulation model. Section 6 selects the model with better performance after comparison under the constraints of engineering practice and optimizes the design. Section 7 summarizes the article and presents the research conclusions.

2. Research process and methods

How to link machine learning with weighted sound insulation in floors becomes key. Data collection and preprocessing may be very tedious, but their importance

cannot be ignored. In this study, the sound insulation data on the floor structure of high-speed trains were obtained through a large number of sound insulation tests. After screening and evaluation, a floor structure sound insulation sample library for subsequent training was established. This was followed by the selection of model inputs. In this process, the physical parameters of the high-speed train floor structure were converted into specific feature parameters. Finally, the model was trained and verified. Once the training data are prepared, different ma-chine learning algorithms can be used to establish the mapping relationship between the feature vector and the target value, that is, the weighted sound insulation R_w of the floor structure, so as to obtain the sound insulation prediction model of the high-speed train's floor structure. The overall research process is shown in **Figure 2**.

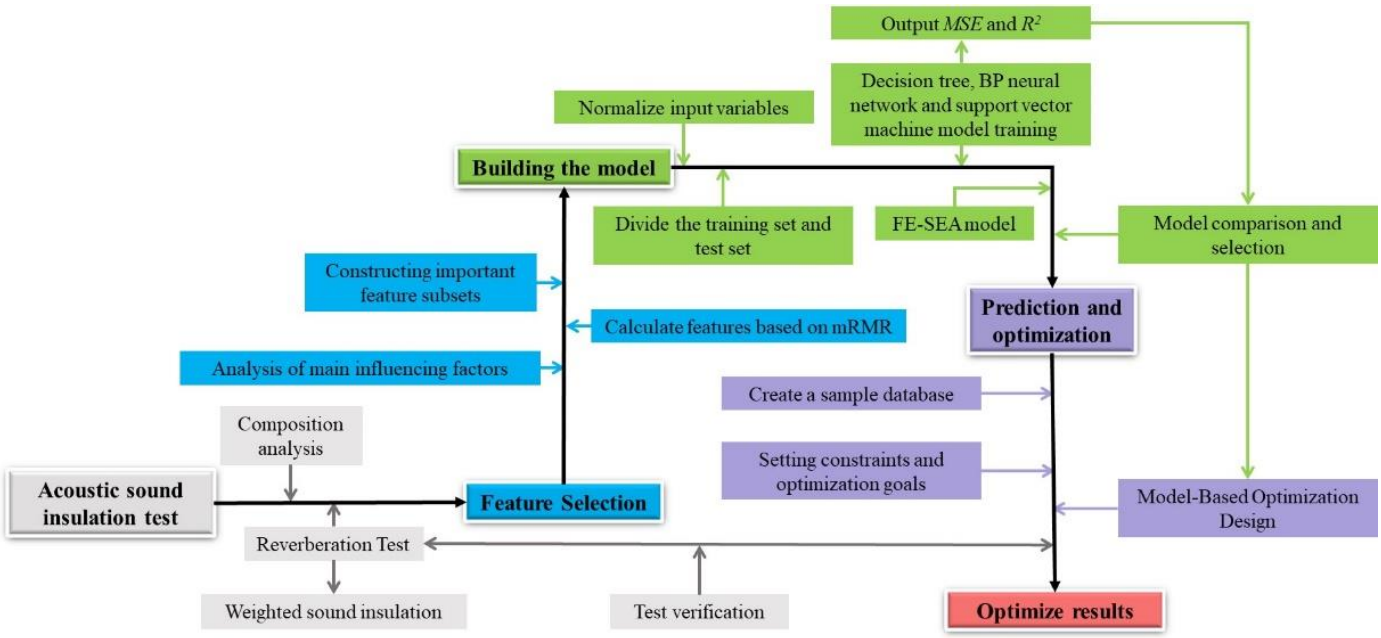

Figure 2. Flowchart of optimization strategy based on machine learning.

3. Sample source, collation, and feature selection

3.1. Sources of test samples, collation

The original data were obtained from a research project on sound insulation of a high-speed train floor structure led by the acoustics laboratory of the Changzhou Institute of Rail Transit Research, China, which aimed to use the acoustics laboratory to study the influence of the wood bone support structure (different wood bone arrangements, different parameters of wood bones and vibration damping pads, etc.) regarding the sound insulation performance of the floor structure. In the project, a total of 97 sets of floor structure test samples were tested for sound insulation characteristics based on the reverberation method [37]. The tests are as follows:

The two reverberation chambers are connected by a 1 m^2 hole for placing the samples to be tested, and the size of the samples is 985 mm × 970 mm. The test of this sample is an effective method for practical applications. It can obtain data that are close to the actual large sample test results. The reliability of the results can be ensured by repeatedly testing different samples. The mutual positions of the sound

isolation samples, sound source, loudspeaker, microphone, and loudspeaker and microphone are based on the ISO10140-2-2021 standard [37]. The experiment was repeated six times to obtain twelve sets of data for averaging. The sample installation and fixing method, including the production of specific devices, specific bolt torque, specific sealing method, etc., are easy to implement. The sample is stable and controllable, and the efficiency of the sound insulation test, the repeatability of the test, and reproducibility of the test results are guaranteed. It is a mature test system. The test site is shown in **Figure 3**.

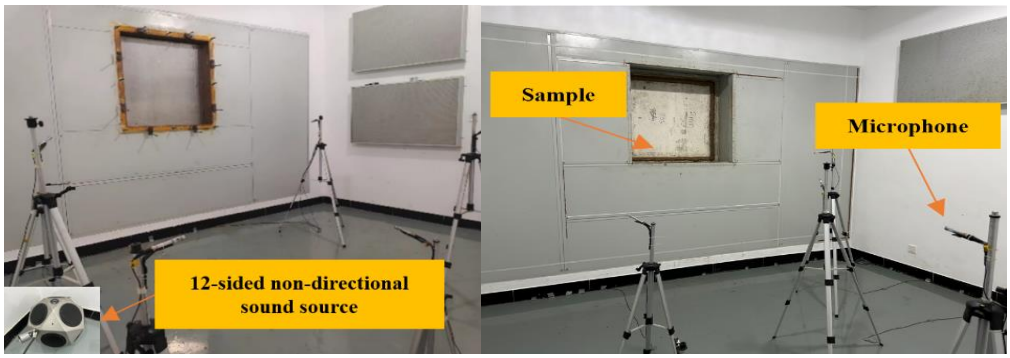

(a) **(b)**

Figure 3. Test site diagram. **(a)** Sound source room; **(b)** Receiving room.

After testing the sound insulation performance of the sample, although the results were not completely consistent with the test results of the large-size sample, they were still highly similar. This method can efficiently and reliably evaluate the sound insulation performance of materials and components under resource-constrained conditions, providing an important reference for the design and optimization of rail transit projects.

We placed the excitation sound sources in the sound source room and the receiving room, respectively, and performed sound pressure level tests on them. The sound insulation level R of the sample can be calculated by substituting Equation (1) into the following:

$$R = L_1 - L_2 + 10\,lg\frac{S}{A} \tag{1}$$

In the formula, L_1 is the average sound pressure level of the sound source room, L_2 is the average sound pressure level of the receiving room, S is the surface area of the sample, and A is the sound absorption coefficient of the receiving room. It can be substituted into Equation (2) to calculate that:

$$A = \frac{0.16V}{T} \tag{2}$$

In the formula, V is the volume of the receiving chamber, and T is the reverberation time of the receiving chamber.

After obtaining the calculation results of the sound insulation frequency curve, the weighted sound insulation level R_w was further calculated according to the standard [38], which was used as a single value evaluation quantity to evaluate the overall sound insulation level of the sample.

The parameters and layout of the wooden bones and vibration damping pads in the wooden bone support structure in the 97 groups of floor test samples are similar. Comparing the sample data with the analysis of the differences in the parameters in the structure, we can roughly analyze the influence of the wooden bone support structure on the overall floor's overall acoustic isolation characteristics, and put forward the idea of directional optimization accordingly.

Table 1. Floor structure composition and selected parameters.

Name		Thickness/mm	Poisson's Ratio	Density (kg/m^3)
Floor cloth		3	0.4896	1100
Inner floor		19.5	0.2500	700
Wooden support structure	Vibration-absorbing pad	/	/	/
	Wooden frame	/	/	/
Sandwich material		40	/	16
Aluminum profile		80	0.3296	2700

Table 2. Samples' wooden support structure parameters.

Structure	Parameter	Sample 1	Sample 2	Sample 3	Sample 4	Sample 5	Sample 6	Sample 7	Sample 8
Vibration-absorbing pad	Density (kg/m^3)	300	640	1150	994	604	645	207	765
	Elastic Modulus (GPa)	1.5	1.9	2.1	1.4	1.1	1.3	2.5	1.2
	Shear modulus (GPa)	0.54	0.70	0.76	0.49	0.38	0.47	0.86	0.41
	Poisson's ratio	0.40	0.35	0.39	0.42	0.45	0.38	0.45	0.46
	Length (mm)	785	330	305	389	225	220	170	118
	Width (mm)	50	50	47	44	44	48	50	43
	Thickness (mm)	12	12	6	6	12	6	12	6
	Quantity	3	6	6	8	9	9	12	12
Wooden frame	Density (kg/m^3)	600	547	505	592	522	598	565	538
	Elastic Modulus (GPa)	12	11.2	12.1	12.4	11.5	12.7	12.6	11.7
	Shear modulus (GPa)	4.80	4.67	4.88	5.00	4.38	5.08	5.04	4.68
	Poisson's ratio	0.25	0.28	0.24	0.24	0.31	0.25	0.25	0.25
	Length (mm)	785	760	380	430	760	240	760	380
	Width (mm)	50	50	50	46	46	50	50	48
	Thickness (mm)	43	43	42	42	43	42	43	40
	Number	3	3	6	8	3	9	3	6

Due to space constraints, this article only provides the composition of eight groups of typical floor structure test samples from the project, as shown in **Tables 1** and **2**. **Table 1** shows the composition of the floor. In this project, the impact of the wooden support structure on its sound insulation was mainly investigated, and the other materials remained unchanged. The wooden support structure included wooden frames and vibration-absorbing pads. The parameters of the wooden support structure in the eight groups of test samples are shown in **Table 2**. In order to help readers quickly and clearly understand the differences between the samples, the

figure shows the wooden support structure of sample 5 and sample 8. **Figure 4** clearly shows the length, width, thickness and number of the vibration damping pad and the wooden frame.

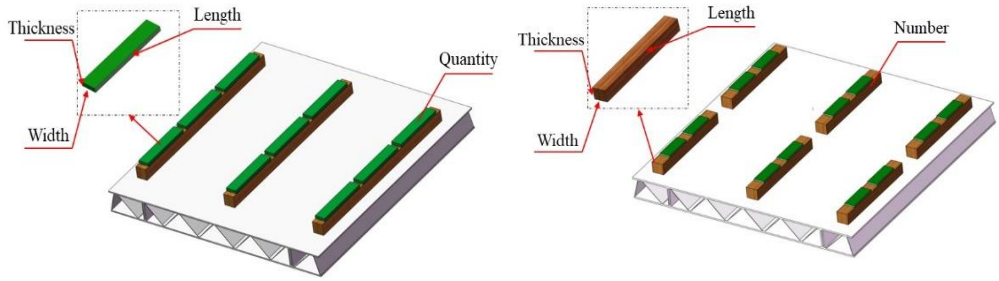

(a) **(b)**

Figure 4. Schematic diagram of wooden frame support structure. **(a)** Sample 5; **(b)** Sample 8.

3.2. Sample feature selection

In machine learning, examining key influencing factors and choosing feature vectors is a crucial step in data preprocessing. Good feature selection can improve the performance of a model, which plays an important role in the further improvement of the model and algorithm. In this paper, based on the results of the project on the sound insulation characteristics of the floor structure of the relevant high-speed train and the measured results of this case, the main influencing factors of the wood bone support structure on the sound insulation characteristics of the floor are analyzed and preprocessed, as described below:

1) Material property parameters: Due to the laboratory conditions and the limitations of the material setting options of the acoustic software, the basic material property parameters mainly include density, modulus of elasticity, Poisson's ratio, and shear modulus. Affected by various wiring harnesses and air ducts, the width of the wooden frame support structure in the manuscript ranges from 42 to 45 mm, and the height ranges from 40 to 45 mm. The layout is a simple horizontally symmetrical arrangement. The density, elastic modulus, and other parameters have a small range of variation, which is determined based on the specific parameters of the upper wooden frame support structure.
2) Acoustic property parameters: The acoustic parameters mainly include the weighted sound insulation amount R_w of a single vibration-absorbing pad and the weighted sound insulation amount R_w of a single wooden frame. Vibration-absorbing pads and wooden frames are components of the wooden support structure, and their respective weighted sound insulation levels R_w are indispensable for evaluating the sound insulation properties of the overall floor.
3) Structural layout attribute parameters: In this project, these parameters mainly includes the weight, length, width, and thickness of the vibration-absorbing pads and wooden frames in the wooden support structure, the number of vibration-absorbing pads, the contact area between the vibration-absorbing pads and the wooden frames, the number of wooden frames, the number of vibration-absorbing pads on the wooden frames, and the contact area between the wood frame and the profile. The above parameters will cause changes in the wooden

support structure, and this change is an important factor affecting the sound insulation properties of the floor's composite structure.

In summary, the characteristic parameters of the above factors were selected and numbered to summarize a total of 23 original characteristic parameters, as shown in **Table 3**.

Table 3. Main influencing factors of wooden support structure.

Serial Number	Influencing Factors	Belongs to	Serial Number	Influencing Factors	Belongs to
F01	Density	Vibration-absorbing pad	F14	Length	Wooden frame
F02	Elastic Modulus	Vibration-absorbing pad	F15	Thickness	Wooden frame
F03	Poisson's ratio	Vibration-absorbing pad	F16	Width	Wooden frame
F04	Length	Vibration-absorbing pad	F17	Sound insulation	Wooden frame
F05	Thickness	Vibration-absorbing pad	F18	Contact area with profile	Wooden frame
F06	Width	Vibration-absorbing pad	F19	Density	Wooden frame
F07	Sound insulation	Vibration-absorbing pad	F20	Elastic Modulus	Wooden frame
F08	Quantity	Vibration-absorbing pad	F21	Poisson's ratio	Wooden frame
F09	Contact area	Vibration-absorbing pad	F22	Weight	Wooden frame
F10	Shear modulus	Vibration-absorbing pad	F23	Shear modulus	Wooden frame
F11	Weight	Vibration-absorbing pad			
F12	Number	Wooden frame			
F13	Number of pads on the wooden frame	Wooden frame			

4. Calculation and significant feature screening based on mRMR

Due to the large number of feature parameters, redundant features should be eliminated before modeling in order to improve the model's quality and computing speed. Therefore, the maximum correlation-minimum redundancy (mRMR) feature selection algorithm for regression data is used [39], which is a feature selection method that is commonly used to deal with high-dimensional data., Tand the core of this algorithm is to select the important features by maximizing the correlation between the features and the target variables while minimizing the redundancy between the features.

The algorithm uses mutual information to measure the correlation between variables. Given two discrete random variables X and Y with their marginal probability distribution functions $p(x)$, and $p(y)$ and joint probability distribution function $p(x,y)$, the mutual information of X and Y is:

$$I(X,Y) = \sum_{x\in X}\sum_{y\in Y} p(x,y)\, log\, \frac{p(x,y)}{p(x)p(y)} \tag{3}$$

Assume that the target feature subset of mRMR is S, the number of features to be selected is m, x_i, x_j ($i, j = 1, 2,\ldots, m, i \neq j$) represent any two features in S, and c represents the target variable. Then, the m features with the greatest correlation with c can be calculated through Equation (4), and the redundancy between the m features can be eliminated through Equation (5).

$$max\ D\ (S,c), D = \frac{1}{S}\sum_{x_i \in S} I(x_i, c) \tag{4}$$

$$min\ R\ (S), R = \frac{1}{|S|^2}\sum_{x_i, x_j \in S} I(x_i, x_j) \tag{5}$$

Combine the maximum correlation *D* with the minimum redundancy *R*, define an operator to combine *D* and *R*, and consider the simplest combination method:

$$max\ \phi\ (D,R), \phi = D - R \tag{6}$$

Finally, the feature set *S* of the maximum correlation minimum redundancy is obtained:

$$mRMR = max\left[\frac{1}{|S|}\sum_{x_i} I(x_i, c) - \frac{1}{|S^2|}\sum_{x_i, x_j \in S} I(x_i, x_j)\right] \tag{7}$$

Use programming software to enter the code and calculate the *maxφ(D,R)* values corresponding to the 23 original characteristic parameters in **Table 3**. The results are shown in **Figure 5**. The numbers of the characteristic parameters in the figure are consistent with those in **Table 3**. Here, *maxφ (D,R)* = 1 is used as the dividing line to distinguish whether a feature is suitable or not. The yellow area in the figure indicates the part where the *maxφ (D,R)* value of each feature exceeds 1. These features will be recognized as suitable features. Salient feature subsets can be stored.

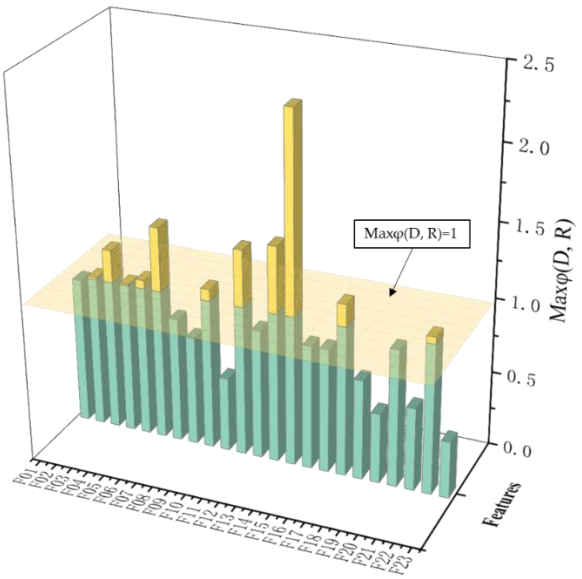

Figure 5. *maxφ (D,R)* calculation result.

The following steps should be considered: (1) Ensure that certain characteristic parameters are screened out. (2) Then compare the solutions and optimize the design. (3) The model's comprehensive coverage of the characteristic parameters and the feasibility of the solution should be assessed. Arrange the feature parameters and

artificially filter out the F20, F15, and F16 feature parameters, store them together as a significant feature subset. In conclusion, the machine learning model identified a subset of significant features comprising 12 parameters, which have been renumbered as detailed in **Table 4**.

Table 4. Salient feature subset.

New Number	Original Number	Influencing Factors	Belongs to
NF01	F14	Length	Wooden frame
NF02	F13	Number of pads on the wooden frame	Wooden frame
NF03	F06	Width	Vibration-absorbing pad
NF04	F11	Weight	Vibration-absorbing pad
NF05	F03	Poisson's ratio	Vibration-absorbing pad
NF06	F09	Contact area with wood frames	Vibration-absorbing pad
NF07	F05	Thickness	Vibration-absorbing pad
NF08	F22	Weight	Wooden frame
NF09	F02	Elastic Modulus	Vibration-absorbing pad
NF10	F20	Elastic Modulus	Wooden frame
NF11	F15	Thickness	Wooden frame
NF12	F16	Width	Wooden frame

5. Predictive modelling, validation, and discussion

5.1. Data standardization

Considering the different units and magnitudes between each feature in the subset of salient features, when the subset of salient features is used as an input variable, it will cause difficulties in terms of the establishment of the model, the speed of operation, and the accuracy of the model, so it is necessary to standardize the data of this subset before establishing the model.

Data standardization is a dimensionless method for processing data characteristics. Dimensionless refers to the need to convert data of different specifications to the same specification, or to convert data of different distributions to a specific distribution. During the model training process, the data characteristics after dimensionality can accelerate the solution of the model.

The Min-Max standardization method is one of the most common data standardization methods. Min-Max normalization performs a linear transformation of the original data and maps the values in the range of between [0,1]. The Min-Max method is applicable to bounded data. and depends on all sample data. The floor data volume in this manuscript is 97, which is a small data set, and the value will not change. Moreover, this manuscript does not involve distance measurements, covariance calculation, etc. The Min-Max method is convenient for eliminating dimensions and incorporating the data of each indicator into the comprehensive evaluation. Therefore, it is preferable reasonable to use the Min-Max method to process the data in this paper. To transform the sample sequence $\{x_1,x_2,x_3,\ldots,x_n\}$, the function is as follows:

$$y_i = \frac{x_i - min_{1\le j\le n\{\mathrm{xj}\}}}{max_{1\le j\le n\{\mathrm{xj}\}} - min_{1\le j\le n\{\mathrm{xj}\}}} \tag{8}$$

In the formula, n is the number of samples. Then, the new sequence y_1, y_2, y_3,..., $y_n \in [0,1]$ is dimensionless.

5.2. Model evaluation

Taking the measured sound insulation data of the aforementioned 97 sets of high-speed train floor combination structures as the total sample, three machine learning models that are commonly used for regression tasks, namely decision tree, the BP neural network model, and the support vector machine regression (SVR) model, were used to analyze prediction of the weighted sound insulation of the high-speed train's composite floor composite structures. Decision trees, BP neural networks, and SVR represent different types of models (tree models, neural networks, and models based on statistical learning), which can provide multi-angle comparison of prediction results. By comparing these three methods, we can have a more comprehensive understanding of the characteristics of the data and its relationship with the prediction results, and provide a reference for selecting appropriate models for future research. For this, 70% (68 groups) of the samples were randomly selected and classified into the training set, and the remaining 30% (29 groups) were classified into the test set for verification. During the verification process, the mean square error (*MSE*) and square correlation coefficient (R^2) were used to evaluate the model's training results. The calculations of *MSE* and R^2 are as follows:

$$MSE = \frac{\sum_{i=1}^{m}(x_i - y_i)^2}{m} \tag{9}$$

$$R^2 = \frac{[\sum_{i=1}^{m}(x_i - \overline{x})(y_i - \overline{y})]^2}{\sum_{i=1}^{m}(x_i - \overline{x})^2 \sum_{i=1}^{m}(y_i - \overline{y})^2} \tag{10}$$

5.3. Decision tree algorithm

Decision tree is a widely used machine learning method that can effectively handle classification and regression problems. Its basic idea is to recursively divide the data set, with each node being a feature, each branch representing the value of the feature, and each leaf node representing a category or a value. Among them, the CART method can effectively model multiple feature variables, and the extraction rules are simple, highly accurate, and easy to understand. The decision tree model is intuitive and easy to understand, and can handle nonlinear relationships. In this context, this paper uses the CART algorithm to predict the sound insulation of high-speed train floors.

Assuming X and Y are input and output variables, forming a training data set, we traverse each feature variable and its corresponding value. Let the current splitting variable be the j-th variable, corresponding to a splitting value s, which can divide and define two regions.

Then, the input space will be continuously divided into L subspaces $\alpha_1, \alpha_2, \ldots, \alpha_L$. Each subspace α_l contains a part of the sample data and output value β_l. The solution of the current model can be expressed as follows:

$$f(x) = \sum_{l=1}^{L} \beta_l I(x \in \alpha_1) \tag{11}$$

The error size of the loss function is compared using the squared error $\sum(y_i - f(x_i))^2$, and the optimal split point and predicted value are determined using the squared error minimization criterion. According to the least squares method, the mean value of all outputs y_i on subspace α_l is the optimal value $\hat{\beta}l$ of β_l, which can be expressed as follows:

$$\hat{\beta}_l = ave(y_i | x_i \in \alpha_l) \tag{12}$$

Select the optimal segmentation attribute j and attribute value s to divide the input space, which is expressed by means of the following formula:

$$\min_{j,s} \left[\min_{\beta_l} \sum_{x_i \in \alpha_1(j,s)} (y_i - \beta_1)^2 + \min_{\beta_2} \sum_{x_i \in \alpha_2(j,s)} (y_i - \beta_2)^2 \right] \tag{13}$$

Traverse all input feature variables and their values, find the current optimal split point (j, s), and then divide the current space into two sub-regions based on the split point. At this time, if the two sub-regions cannot be divided, the corresponding optimal output value can be obtained, expressed as follows:

$$\begin{cases} \hat{\beta}_1 = ave(y_i | x_i \in \alpha_1(j,s)) \\ \hat{\beta}_2 = ave(y_i | x_i \in \alpha_2(j,s)) \end{cases} \tag{14}$$

According to the above steps, if the division can continue, repeat the above steps until it stops.

Figure 6a below shows the comparison between the actual measurements and the prediction results of the training set. It can be seen that the actual measurements and the prediction results of the training set are relatively close. Their *MSE* is 0.015673, and R^2 is 0.94075. The effect of the model training is good.; Further, **Figure 6b** shows the comparison between the actual measurement and prediction results of the test set, but the consistency between the measurement and prediction results is not high. Its *MSE* is 0.12145, and R^2 is 0.60359, indicating that the trained model is not effective. Subsequent adjustments and retraining should be carried out.

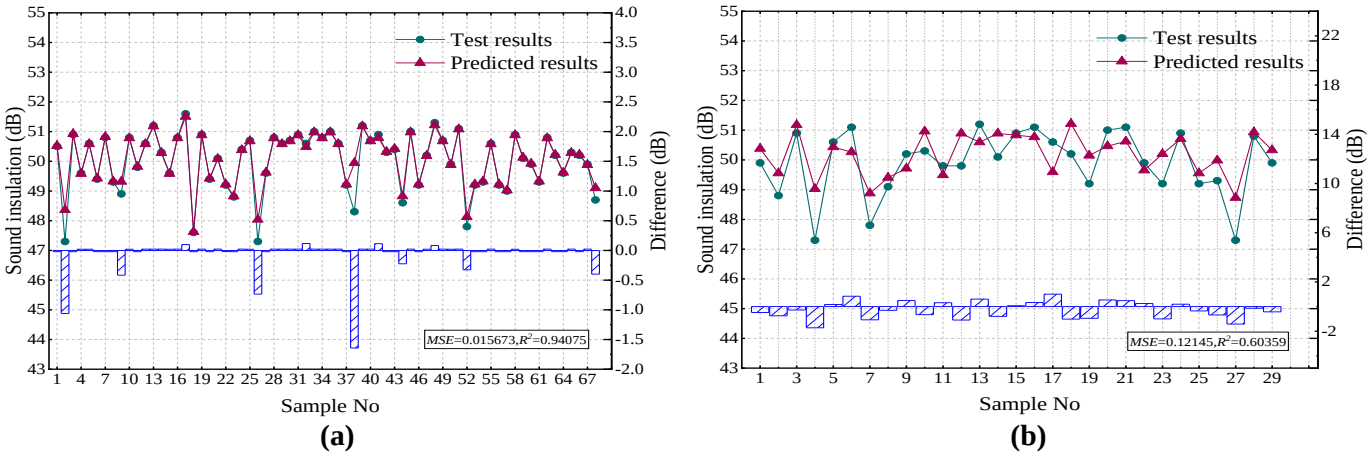

Figure 6. Comparison of actual measurements and prediction results. **(a)** Training set; **(b)** Test set.

5.4. BP neural network method

A BP neural network (BPNN, Back Propagation Neural Network) can essentially be considered a simplified biological model. The data are first imported into the input layer and then passed to the hidden layer. For the hidden layer, the received signal will be passed to the output layer again according to certain rules according to the weight of the interconnected neurons. The output layer will compare the results. If there is an error, it will return to modify the weight of the interconnected neurons. It is good at handling complex pattern recognition problems, especially performing well in nonlinear and high-dimensional data, can automatically learn features, and has strong generalization ability. Its structural model is shown in **Figure 7**.

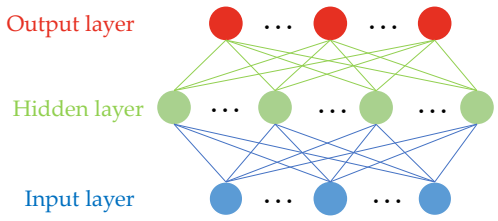

Figure 7. Structural model diagram.

Before training, the variables of the input layer, hidden layer, and output layer must be defined, and each variable must be initialized. The number of nodes is set to *a*, *b*, and *c*, respectively, the connection weight values between each layer are set to ω_{ij} and ω_{jk}, respectively, and the neuron transfer function is selected. Calculate the output value H of the hidden layer according to Equation (15):

$$H_j = f\left[\sum_{n}^{i=1}(\omega_{ij} - \alpha_j)\right]; j = 1,2,\ldots,b \tag{15}$$

According to Equation (16), calculate the predicted output *O*:

$$O_k = \sum_{j}^{1} H_j\omega_{jk} - b_k; k = 1,2,\ldots,c \tag{16}$$

Based on the predicted output O and the actual output Y, calculate the loss function e:

$$e^k = Y_k - O_k; k = 1,2,\ldots,c \tag{17}$$

According to the back propagation error, adjust the correction weights ω_{ij}, ω_{jk}, and p,t. Finally, check whether the error evaluation training of the output value is qualified. When the error reaches the minimum, the training stops. If the error value can continue to decrease, return to continue training.

A neural network model was established using MATLAB2016b software. The specific neural network model implementation process is shown in **Figure 8**.

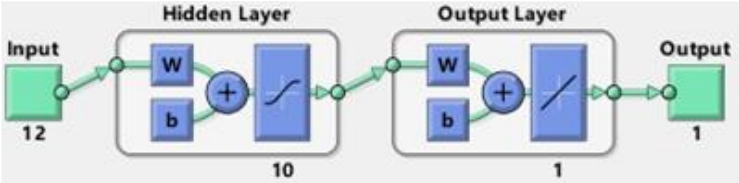

Figure 8. Neural network model implementation process.

Figure 9a shows the comparison between the measured and predicted results of the 68 samples in the training set. It can be seen that the *MSE* is 0.015673 and the R^2 is 0.94075. The two curves of the actual measured value and the predicted value of the training set are in good agreement, which shows that the model training effect is better; **Figure 9b** shows the comparison between the actual measurement and prediction results of the 29 samples in the test set. The *MSE* is 0.018782, R^2 is 0.87628, and the model is relatively stable.

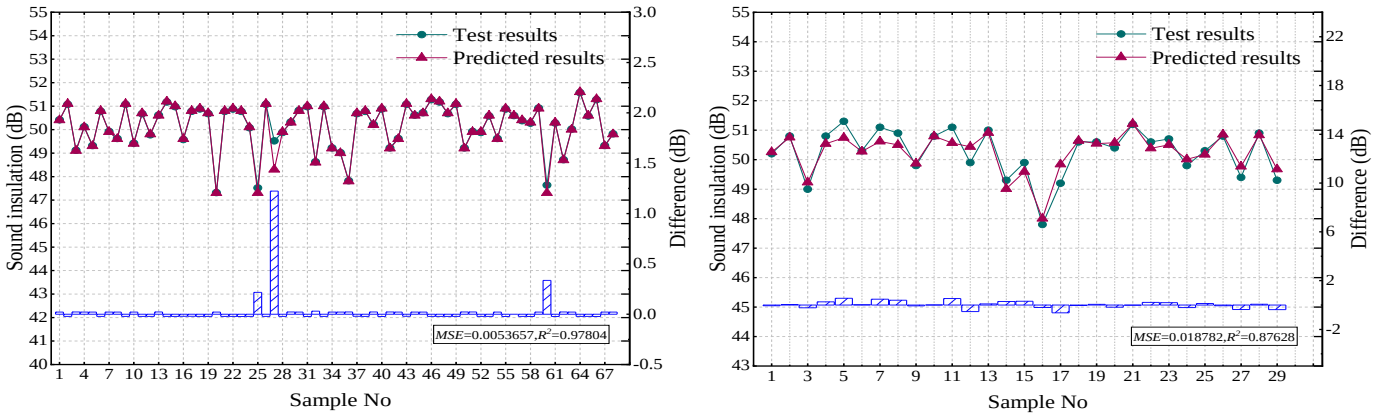

(a) **(b)**

Figure 9. Comparison of actual measurements and prediction results. **(a)** Training set; **(b)** Test set.

5.5. Support vector machine regression (SVR) method

Support vector regression (SVR) is a regression method based on the support vector machine (SVM). Different from traditional regression methods, the goal of SVR is not to directly fit the data, but to find a hyperplane in the feature space so that the sample points are as close to the hyperplane as possible, and a certain error is allowed within the tolerance range. SVR performs well in processing high-

dimensional data and has good generalization ability, especially in the case of small samples, and can effectively avoid overfitting problems.

For the regression problem, given the training data set $D = \{(x_1,y_1),(x_2,y_2),\ldots,(x_i,y_i)\}$, where $x_i \in R^n$ is the n-dimensional input sample and $y_i \in R$ is the output sample, the aim is to learn a regression model $f(x) = w^T x + b$ so that $f(x)$ and y are as close as possible. w and b are model parameters.

For samples (x, y), traditional regression models usually calculate the loss directly based on the difference between the model output $f(x)$ and the true output y. The loss is 0 if and only if $f(x)$ is exactly the same as y. In contrast to this, the support vector machine (SVR) assumes that we can tolerate up to ε errors between $f(x)$ and y, and only calculates the loss when the absolute value of the difference between $f(x)$ and y is greater than ε.

Therefore, the SVR problem is written as follows:

$$\min_{w,b} \frac{1}{2}\|w\|^2 + C\sum_{i=1}^{m} l_\varepsilon\left(f(x_i) - y_i\right) \tag{18}$$

In the formula, C is a regularization constant. We introduce the slack variables ξ_i and $\hat{\xi}_i$, rewrite the above formula, and satisfy the constraints:

$$\min_{w,b,\xi_i,\hat{\xi}_i} \frac{1}{2}\|w\|^2 + C\sum_{i=1}^{m}(\xi_i,\hat{\xi}_i) \tag{19}$$

$$\left.\begin{aligned} &s.t.\mathrm{f}(x_i) - y_i \le \varepsilon + \xi_i \\ &y_i - f(x_i) \le \varepsilon + \hat{\xi}_i \\ &\xi_i \ge 0, \hat{\xi}_i \ge 0, i = 1,2,\ldots,m \end{aligned}\right\} \tag{20}$$

Furthermore, the SVR dual problem is obtained:

$$\max_{\alpha,\hat{a}} \sum_{i=1}^{m} y_i(\hat{\alpha}_i - \alpha_i) - \varepsilon(\hat{\alpha}_i + \alpha_i) - \frac{1}{2}\sum_{i=1}^{m}\sum_{j=1}^{m}(\hat{\alpha}_i - \alpha_i)(\hat{\alpha}_i + \alpha_i)x_i^T x_j \tag{21}$$

$$\left.\begin{aligned} &s.t.\sum_{i=1}^{m}(\hat{\alpha}_i - \alpha_i) = 0 \\ &0 \le \hat{\alpha}_i, \alpha_i \le C, i = 1,2,\ldots,m \end{aligned}\right\} \tag{22}$$

The above process satisfies the KKT condition. Then, we map the data to a high-dimensional feature space for linear regression, use the kernel function to replace the inner product operation in the linear problem, replace x with $\varphi(x)$, and obtain the final model of the support vector machine:

$$f(x) = \sum_{i=1}^{m}(\hat{\alpha}_i - \alpha_i)\varphi(x_i)^T\varphi(x_i) + b \tag{23}$$

Figure 10a shows the comparison between the actual measurements and the prediction results of the 68 samples in the training set. It can be seen that the *MSE* is 0.00009724 and the R^2 is 0.99976. The two curves of the actual measured value and

the predicted value of the training set are in good agreement, which shows that the model training effect is better; **Figure 10b** shows the comparison between the measured and predicted results for the 29 samples in the test set. It can be seen that the measured and predicted values in the test set are still highly consistent, with an *MSE* of 0.009842 and an R^2 of 0.96782. This shows that the trained model has good generality. In addition, during the operation process, the training set and test set are randomly selected, so the trained model has a certain degree of randomness. The above shows that the SVR model is reliable for subsequent numerical predictions.

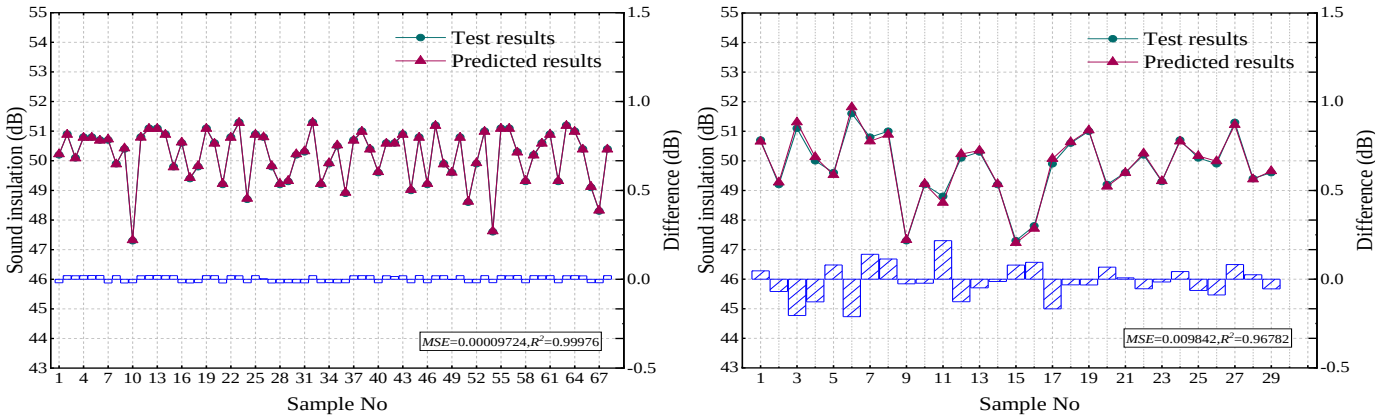

Figure 10. Comparison of actual measurements and prediction results. **(a)** Training set; **(b)** Test set.

5.6. Comparison and discussion of machine learning models

In order to optimize the wooden support structure below the floor, the *MSE* and R^2 of the prediction sets of the above three machine learning prediction models are now compared, as shown in **Figure 11**. Numbers 1, 2, and 3 represent the decision tree, BP neural network, and SVR. The two curve trends in the figure show that among the models trained in this article, SVR has a better effect.

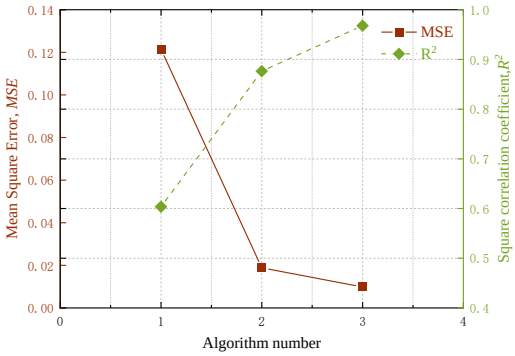

Figure 11. Comparison of prediction sets' evaluation criteria.

In addition, cross-validation is a technique for evaluating the performance of statistical models (such as machine learning models). It is mainly used to evaluate the performance of a model on independent data sets, avoid overfitting, and ensure the generalization ability of the model.

Based on the idea of cross-evidence, the SVR model was used as an example. From this, 70% (68 groups) of the questions were taken as practice tests and the

remaining 30% (29 groups) were taken as test questions. We repeated the process 20 times to statistically calculate the *MSE* and R^2 values for each training and measurement set, as shown in **Figure 12**. As can be seen in **Figure 12a**, the *MSE* of the 20 training sets was between 0 and 0.02, the R^2 was between 0.9 and 1.0, and most were close to 1. As can be seen in **Figure 12b**, the *MSE* of the corresponding measurements ranged from 0 to 0.06 and was often around 0.02, and the R^2 ranged from 0.8 to 1.0. In general, the model was more powerful.

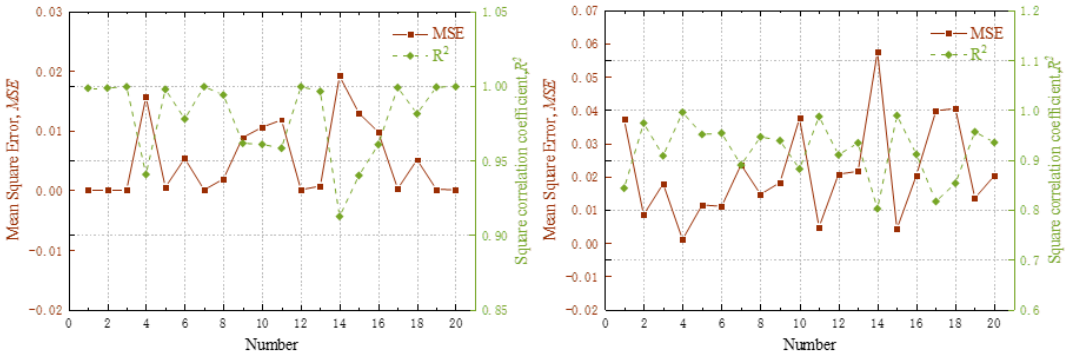

Figure 12. *MSE* and R^2 values for the floor structure diagram. **(a)** Test results; **(b)** Predicted results.

Further, the prediction models are compared and discussed in terms of prediction accuracy. As shown in **Figure 13**, the material composition of the composite structure of a new high-speed train floor developed in this project, is shown. Taking this floor combination structure as an example, we use the trained model to predict the weighted sound insulation level, and compare the predicted results with the measured sound insulation results of the reverberation method in Section 3.1. In addition, the FE-SEA method (**Figure 14**) is also used to conduct sound insulation modeling and simulation of the floor structure. FE-SEA simulations provide an independent data source, allowing us to more fully evaluate the performance of the model.

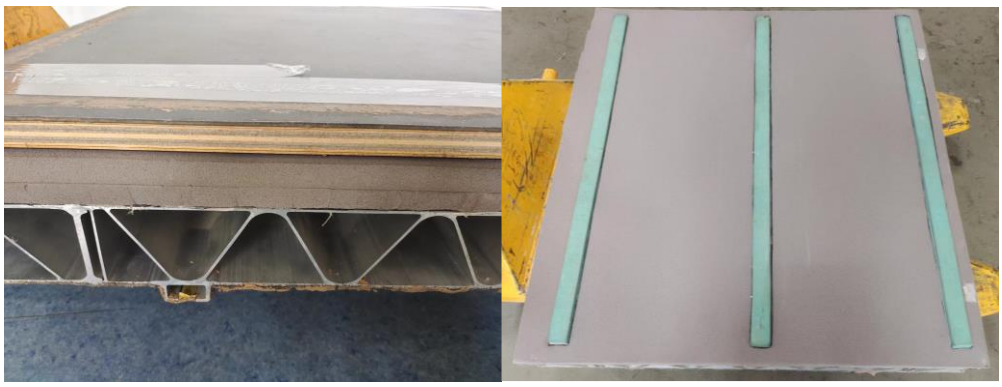

Figure 13. Floor structure diagram. **(a)** Cross-sectional photography; **(b)** Distribution diagram of wooden support structure.

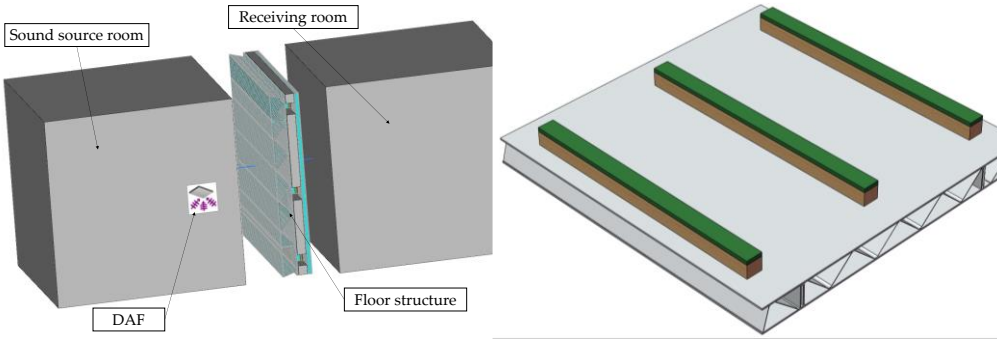

(a) **(b)**

Figure 14. Predictive model diagram. **(a)** FE-SEA prediction model; **(b)** Distribution diagram of wooden support structure.

Table 5 shows the comparison between the predicted values of the above prediction methods and the actual measured values. It can be seen that the predicted value of the weighted sound insulation R_w based on the support vector machine regression method only differs from the measured value by 0.3 dB, which is compared with the 1.6 dB of the hybrid FE-SEA model, the 0.5 dB of the BP neural network, and the 1.1 dB of the decision tree error. The accuracy has been significantly improved. Finally, in the prediction task of this article, the support vector machine regression (SVR) method is the most suitable prediction model for the optimization of the wooden support structure.

Table 5. Comparison of different model predictions and actual measurement results.

Method of Prediction	Model Category	Weighted Sound Insulation R_w/dB	Error/dB
Experiment	Reverberation method test	50.7	/
Simulation	Hybrid FE-SEA	49.1	1.6
Machine learning	Decision tree	49.6	1.1
Machine learning	BP neural network	51.2	0.5
Machine learning	SVR	51.0	0.3

6. Target optimization based on engineering practice

6.1. Optimization goals and constraints

Due to the influence of the material type, quantity, cost, construction period, and other conditions, only 97 sound insulation tests of high-speed train floor structure samples were completed in this project. However, for machine learning, the number of experimental results is still very small, which can only guide directional optimization ideas to a certain extent, and cannot determine the optimal structural solution. This section mainly uses the prediction model of the support vector machine regression method, which was previously shown to have a good training effect, to seek the rapid prediction of the optimal plan for the wooden support structure and its related parameters, and complete the optimization with the main goal of sound insulation of the floor structure.

Overall, sound insulation is the acoustic design goal of the floor structure. Combined with the actual engineering and the main research object of this article

(a wooden support structure), and based on the project's design goals and planning, this section uses the overall thickness and density of the wooden support structure of the design plan as "constraints". The specific description of these "constraints" is as follows:

1) Overall thickness: The floor structure will be subject to conditions during assembly. As a component of the floor structure, the overall thickness of the wooden support structure will also be limited. Therefore, the overall thickness of the timber support structure serves as one of the "constraints".
2) Overall density: Lightweighting high-speed trains is an important measure to reduce the demand for traction power of high-speed EMUs and achieve high-speed operation. It improves the operating efficiency and reduces energy consumption. and is a key development trend for high-speed trains. Therefore, the overall density of the wooden support structure serves as one of the "constraints".

6.2. Optimization implementation and analysis

Based on the comparative evaluation of the machine learning model in Section 5.6, this section will optimize the wooden support structure and illustrate the beneficial effect of the SVR model on target optimization.

First, the salient characteristic parameters and their specific data that were screened out in **Table 4** are sorted. It should be noted that there are restrictions on some parameters in the optimization of this project, so the salient characteristic parameters and their values that meet the requirements of this project are used to form a new sample library.

Furthermore, by permuting and combining the calculation results, it can be seen that the number of possible solutions is $N = 26357760$. However, it should be noted that among such a large number of solutions, not all solutions are reasonable or meet the actual assembly requirements. The reasons for this are as follows:

1) The number of damping pads on a single wooden frame multiplied by the length of a single damping pad should not be greater than the length of a single wooden frame.
2) The width of the vibration-absorbing pad should not be greater than the width of the wooden frame.

Therefore, all solutions that are unreasonable or do not meet the feasibility of assembly are eliminated. After elimination, the SVR prediction model is used to calculate all the solutions, so as to obtain the predicted value of the sound insulation level for each solution, and, under the "constraint conditions", find the best solution to achieve project feasibility.

After evaluating and screening, 303,696 solutions were identified that satisfy all the constraints and assembly requirements, given that the overall thickness of the wooden support structure was 60 mm and the solution's density did not exceed 1000 kg/m^3. **Figure 15** depicts a scatter plot of these floor structure configurations, where the x, y, and z axes represent the density, total thickness, and weighted sound insulation of each scheme, respectively. The

scheme that achieved the maximum sound insulation of 50.45 dB is highlighted in the figure. The specific values of the significant characteristic parameters corresponding to this scheme are given, as shown in **Table 6**.

Table 6. Structural parameters of the maximum sound insulation plan.

Structure	Parameter	Value
Vibration-absorbing pad	Density (kg/m^3)	500
	Elastic Modulus (GPa)	2
	Length (mm)	500
	Width (mm)	40
	Thickness (mm)	12
	Poisson's ratio	0.43
Wooden frame	Density(kg/m^3)	1275
	Elastic Modulus (GPa)	12.5
	Thickness (mm)	42.6
	Width (mm)	44
	Length (mm)	785
	Number of pads on the wooden frame	1

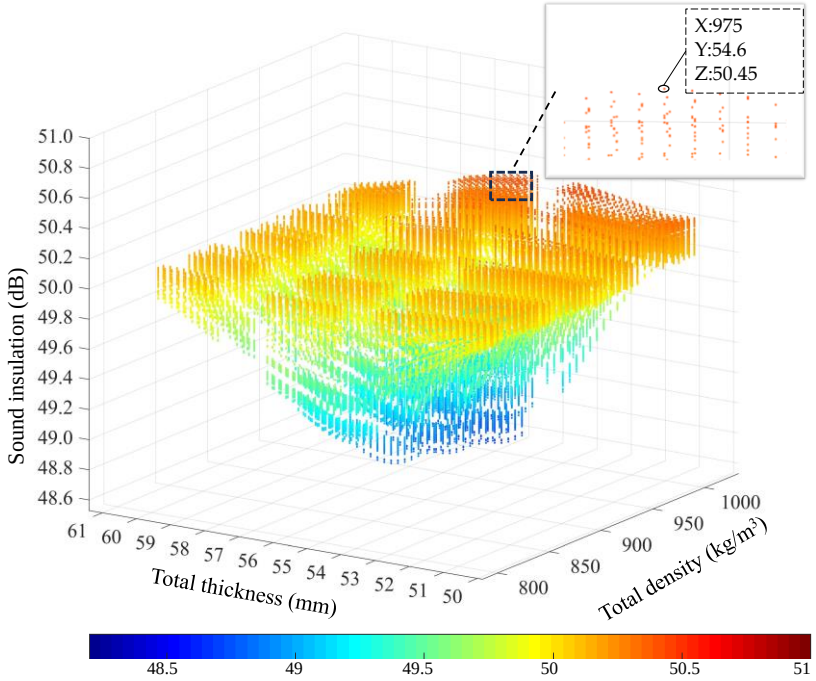

Figure 15. Calculation results of solutions that meet the conditions.

The highest-performing sound insulation solution achieves an overall density that adheres to the weight requirement of not exceeding 1000 kg/m^3; the thickness of the wooden frames is 42.6 mm, the thickness of the vibration-absorbing pad is 12 mm, and the overall thickness of the wooden support structure is 54.6 mm, which meets the project requirements. Based on the preceding analysis, the obtained solution satisfies all the limiting conditions and

is a feasible solution. In addition, through the reverberation method's test verification, the weighted sound insulation of this scheme is found to be 50.55 dB, and the error is only 0.1 dB, indicating that the optimization results are reasonable and accurate.

7. Conclusions

Through this research, the sound insulation performance of a high-speed train's floor has successfully been improved. First, the data required for model training were obtained and organized based on the reverberation test method, and feature selection was performed. Then, the maximum mutual information minimum redundancy (mRMR) algorithm was used to screen out the significant feature subsets. Subsequently, the decision tree, BP neural network, and support vector machine regression (SVR) methods were applied, and the standardized feature data were used for the high-speed train floor timber support structure under the same evaluation criteria of mean square error (*MSE*) and coefficient of determination (R^2). Training and validation of the sound insulation prediction models were carried out. In engineering practice, the SVR model can effectively optimize the wooden support structure in the floor structure under certain constraints. The main conclusions are as follows:

(1) The maximum mutual information minimum redundancy (mRMR) algorithm is used to calculate the selected features and screen out a subset of significant features, which provides strong support for the subsequent model training.

(2) The comparative results show that the prediction errors of the decision tree model, BP neural network model, and finite element statistical energy analysis (FE-SEA) model are 1.1 dB, 0.5 dB, and 1.6 dB. The prediction error of the SVR model is only 0.3 dB, which is significantly better than the above model, indicating that the SVR model has higher reliability and prediction accuracy.

(3) According to the planning of a certain project, the SVR model was used to optimize the design under certain constraints, and we successfully optimized the wooden support structure in the floor. The prediction results show that the weighted sound insulation of the overall floor reaches 50.45 dB, which reflects the significant application value and practical feasibility of the SVR model in engineering practice.

As the number of samples increases, the performance of the model will be further improved, and the prediction results will be more accurate.

Author contributions: Writing—original draft, HD; supervision, RW and XZ; methodology, ZX, AZ and LX; experiment, ZX, AZ and LX; validation, RW; writing—review and editing, RW. All authors have read and agreed to the published version of the manuscript.

Funding: This research was funded by [Changzhou Applied Basic Research Project] grant number [CJ20241064].

Acknowledgments: The authors would like to express their gratitude to the editors and anonymous reviewers for their comments and suggestions.

Availability of data and materials: The data underlying this article cannot be shared publicly due to the privacy of individuals that participated in the study. The data will be shared on reasonable request to the corresponding author.

Conflict of interest: The authors declare no conflict of interest.

References

1. Jin, X. (2018). Key problems faced in high-speed train operation. China's High-Speed Rail Technology: An International Perspective, 27-45. https://doi.org/10.1007/978-981-10-5610-9_2.
2. Park, B., Jeon, J. Y., Choi, S., Park, J. (2015). Short-term noise annoyance assessment in passenger compartments of high-speed trains under sudden variation. Applied Acoustics, 97, 46-53. https://doi.org/10.1016/j.apacoust.2015.04.007.
3. Zhang, J., Han, G., Xiao, X., Wang, R., Zhao, Y., Jin, X. (2018). Influence of wheel polygonal wear on interior noise of high-speed trains. China's High-Speed Rail Technology: An International Perspective, 373-401. https://doi.org/10.1631/jzus.A1400233.
4. Liu, C., Ma, K., Zhu, T., Ding, H., Sun, M., Wu, P. (2024). A New Car-Body Structure Design for High-Speed EMUs Based on the Topology Optimization Method. Applied Sciences, 14(3), 1074. https://doi.org/10.3390/app14031074.
5. Thompson, D., Kouroussis, G., Ntotsios, E. (2019). Modelling, simulation and evaluation of ground vibration caused by rail vehicles. Vehicle System Dynamics, 57(7), 936-983.https://doi.org/10.1080/00423114.2019.1602274.
6. Hardy, A. (1999). Railway passengers and noise. Proceedings of the Institution of Mechanical Engineers, Part F: Journal of Rail and Rapid Transit, 213(3), 173-180. https://doi.org/10.1243/0954409991531128.
7. Thompson, D., Jones, C. (2000). A review of the modelling of wheel/rail noise generation. Journal of sound and vibration, 231(3), 519-536. https://doi.org/10.1006/jsvi.1999.2542.
8. Noh, H. (2017). Contribution analysis of interior noise and floor vibration in high-speed trains by operational transfer path analysis. Advances in Mechanical Engineering, 9(8), 1687814017714986. https://doi.org/10.1177/1687814017714986.
9. Hu, Y., Nakao, T., Nakai, T., Gu, J., Wang, F. (2005). Vibrational properties of wood plastic plywood. Journal of Wood Science, 51, 13-17. https://doi.org/10.1007/s10086-003-0624-9.
10. Jiang, S., Yang, S., Zhang, B., Wen, B. (2019). Experimental and numerical investigation on the external aerodynamic noise of high-speed train. Sound & Vibration, 53(4), 129-138. https://doi.org/10.32604/sv.2019.04048.
11. Shi, J., Zhang, J. (2024). Effect of bogie cavity end wall inclination on flow field and aerodynamic noise in the bogie region of high-speed trains. Computer Modeling in Engineering & Sciences, 139(2), 2175-2195. https://doi.org/10.32604/cmes.2023.043539.
12. Sadri, M., Brunskog, J., Younesian, D. (2016). Application of a Bayesian algorithm for the Statistical Energy model updating of a railway coach. Applied Acoustics, 112, 84-107.https://doi.org/10.1016/j.apacoust.2016.05.014.
13. Han, Y., Sun, W., Zhou, J., Gong, D. (2019). Vibration Analysis of Composite Multilayer Floor of High-Speed Train. Shock and Vibration, 2019(1), 6276915. https://doi.org/10.1155/2019/6276915.
14. Kim, S., Seo, T., Kim, J., Song, D. (2011). Sound-insulation design of aluminum extruded panel in next-generation high-speed train. Transactions of the Korean Society of Mechanical Engineers A, 35(5), 567-574. https://doi.org/10.3795/KSME-A.2011.35.5.567.
15. Wang, R., Yao, D., Zhang, J., Xiao, X., Jin, X. (2023). Effect of the laying order of core layer materials on the sound-insulation performance of high-speed train carbody. Materials, 16(10), 3862. https://doi.org/10.3390/ma16103862.
16. Zhang, J., Yao, D., Wang, R., Xiao, X. (2021). Vibro-acoustic modelling of high-speed train composite floor and contribution analysis of its constituent materials. Composite Structures, 256, 113049. https://doi.org/10.1016/j.compstruct.2020.113049.
17. Yao, D., Zhang, J., Wang, R., Xiao, X. (2021). Vibroacoustic damping optimisation of high-speed train floor panels in low- and mid-frequency range. Applied Acoustics, 174: 107788. https://doi.org/10.1016/j.apacoust.2020.107788.
18. Maknickas, A., Ardatov, O., Bogdevičius, M., & Kačianauskas, R. (2022). Modelling the interaction between a laterally deflected car tyre and a road surface. Applied Sciences, 12(22), 11332. https://doi.org/10.3390/app122211332.

19. Liu, J., Yu, M., Chen, D., Yang, Z. (2022). Study on interior aerodynamic noise characteristics of the high-speed maglev train in the low vacuum tube. Applied Sciences, 12(22), 11444. https://doi.org/10.3390/app122211444.
20. Peng, C., Cheng, S., Sun, M., Ren, C., Song, J. et al. (2024). Prediction of sound transmission loss of vehicle floor system based on 1d-convolutional neural networks. Sound & Vibration, 58(1), 25-46. https://doi.org/10.32604/sv.2024.046940.
21. Panahi, E., Hosseinkhani, A., Frangi, A., Younesian, D., Zega, V. (2022). A novel low-frequency multi-bandgaps metaplate: Genetic algorithm based optimization and experimental validation. Mechanical Systems and Signal Processing, 181, 109495. https://doi.org/10.1016/j.ymssp.2022.109495.
22. Wu, L., Zhai, Z., Zhao, X., Tian, X., Li, D., Wang, Q., et al. (2022). Modular design for acoustic metamaterials: low-frequency noise attenuation. Advanced Functional Materials, 32(13), 2105712. https://doi.org/10.1002/adfm.202105712.
23. Li, Z., Ma, T., Wang, Y., Chai, Y., Zhang, C., Li, F. (2022). Active auto-adaptive metamaterial plates for flexural wave control. International Journal of Solids and Structures, 254, 111865.https://doi.org/10.1016/j.ijsolstr.2022.111865.
24. Liu, Z., Xu, H., Zhu, P. (2020). An adaptive multi-fidelity approach for design optimization of mesostructure-structure systems. Structural and Multidisciplinary Optimization, 62(1), 375-386.https://doi.org/10.1007/s00158-020-02501-x.
25. Zhang, J., Xiao, X., Sheng, X., Zhang, C., Wang, R., Jin, X. (2016). SEA and contribution analysis for interior noise of a high speed train. Applied Acoustics, 112, 158-170. https://doi.org/10.1016/j.apacoust.2016.05.019.
26. Xie, G., Thompson, D., Jones, C. (2006). A modelling approach for the vibroacoustic behaviour of aluminium extrusions used in railway vehicles. Journal of Sound and Vibration, 293(3-5), 921-932. https://doi.org/10.1016/j.jsv.2005.12.015.
27. Cotoni, V., Langley, R., Shorter, P. (2008). A statistical energy analysis subsystem formulation using finite element and periodic structure theory. Journal of sound and Vibration, 318(4-5), 1077-1108.https://doi.org/10.1016/j.jsv.2008.04.058.
28. Kim, K., Lee, J., Kim, D. (2012). A study on the vibroacoustic analysis of aluminum extrusion structures. Comput Aided Des Appl PACE, 2, 1-8. https://doi.org/10.3722/CADAPS.2012.PACE.1-8.
29. Yu, Y., Xiao, X., Wang, D., Wang, H. (2011). Prediction of interior structure borne noise of a cabin of high speed train using FE-SEA hybrid methods. In INTER-NOISE and NOISE-CON Congress and Conference Proceedings (Vol. 2011, No. 4, pp. 3073-3078). Institute of Noise Control Engineering.
30. Yan, G., Li, Y., Huang, X., Yao, S., Zhou, W. (2023). Multi-objective optimization of elastic metaplates for lightweight and ultrawide bandgaps. International Journal of Mechanical Sciences, 259, 108603. https://doi.org/10.1016/j.ijmecsci.2023.108603.
31. Li, M. (2018). A study on the influence of non-intelligence factors on college students' English learning achievement based on C4. 5 algorithm of decision tree. Wireless Personal Communications, 102(2), 1213-1222. https://doi.org/10.1007/s11277-017-5177-0.
32. Doksoo, L.; Chen, W.; Wang, L.-W.; Chan, Y.-C. Data-Driven Design for Metamaterials and Multiscale Systems: A Review. Adv. Mater. 2024, 36, 2305254. https://doi.org/10.1002/adma.202305254.
33. Zheng, X., Zhang, X., Chen, T., Watanabe, I. (2023). Deep learning in mechanical metamaterials: from prediction and generation to inverse design. Advanced Materials, 35(45), 2302530. https://doi.org/10.1002/adma.202302530.
34. Carleo, G., Troyer, M. (2017). Solving the quantum many-body problem with artificial neural networks. Science, 355(6325), 602-606. https://doi.org/10.1126/science.aag2302.
35. Wang, R., Yao, D., Zhang, J., Xiao, X., Xu, Z. (2023). Identification of Key Factors Influencing Sound Insulation Performance of High-Speed Train Composite Floor Based on Machine Learning. Acoustics.6,1-17. https://doi.org/10.3390/acoustics6010001.
36. Sahib, M., Kovács, G. (2023). Elaboration of a multi-objective optimization method for high-speed train floors using composite sandwich structures. Applied Sciences, 13(6), 3876.https://doi.org/10.3390/app13063876.
37. ISO (2021). ISO 10140-2:2021; Acoustics—Laboratory Measurement of Sound Insulation of Building Elements—Part 2: Measurement of Airborne Sound Insulation. ISO: Geneva, Switzerland.
38. ISO (2013). ISO 717–1:2013; Acoustics—Rating of Sound Insulation in Buildings and of Building Elements—Part 1: Airborne Sound Insulation. ISO: Geneva, Switzerland.
39. Peng, H., Long, F., Ding, C. (2005). Feature selection based on mutual information criteria of max-dependency, max-relevance, and min-redundancy. IEEE Transactions on pattern analysis and machine intelligence, 27(8), 1226-1238. https://doi.org/10.1109/TPAMI.2005.159.